Tumor Imaging Agents

A Labeled Neutral Endopeptidase Inhibitor as a Potential Tool for Tumor Diagnosis and Prognosis**

Olivier Raguin, Marie-Claude Fournié-Zaluski, Anthony Romieu, André Pèlegrin, François Chatelet, Didier Pélaprat, Jacques Barbet, Bernard P. Roques, and Anne Gruaz-Guyon**

Scintigraphy with labeled somatostatin analogues and positron-emission tomography (PET) with ^{18}F-labeled 2-deoxy-2-fluoro-D-glucose (^{18}F-FDG) have greatly improved the diagnosis and staging of numerous tumors with somatostatin-receptor-subtype overexpression or active glucose metabolism, respectively. This entailed the development of numerous radiolabeled peptides that target other receptors overexpressed by tumors that do not accumulate somatostatin analogues or ^{18}F-FDG.[1,2] Proteolytic enzymes expressed on many cancer cells are also potential targets for radiopharmaceuticals. Recently ^{18}F- or ^{11}C-labeled inhibitors of metalloproteinase-2 (MMP-2), which is expressed in a variety of malignant tumors, have been proposed for use in PET.[3,4]

Neutral endopeptidase (NEP, CD10, CALLA, enkephalinase, neprylisin, EC 3.4.24.11) is a membrane-bound zinc metallopeptidase that interrupts cell signaling by degradation

[*] Dr. A. Romieu, Prof. B. P. Roques
INSERM U266
Université Paris V René Descartes
4 avenue de l'Observatoire, 75006 Paris (France)
Fax: (+33) 1-4326-6918
E-mail: roques@pharmacie.univ-paris5.fr

Dr. O. Raguin,[+] Dr. D. Pélaprat,[+] Dr. A. Gruaz-Guyon[+]
EA 3512, Faculté de Médecine Xavier Bichat
BP416, 16 rue Henri Huchard, 75870 Paris cedex 18 (France)
Fax: (+33) 1-4485-6306
E-mail: gruaz@bichat.inserm.fr

Prof. M.-C. Fournié-Zaluski
Pharmaleads
4 avenue de l'Observatoire, 75270 Paris cedex 06 (France)

Dr. A. Pèlegrin[+]
INSERM EMI 0227, Université Montpellier 1
CRLCC Val d'Aurelle
Centre de Recherche en Cancérologie
34298 Montpellier cedex 5 (France)

Prof. F. Chatelet
UFR Saint-Antoine, Université Paris VI Pierre et Marie Curie
27 rue Chaligny, 75012 Paris (France)

Dr. J. Barbet[+]
INSERM U601, Université de Nantes
Institut de Biologie
9 quai Moncousu, 44093 Nantes cedex 01 (France)

[+] These authors are members of the CNRS GDR 2352, Immunociblage des tumeurs, Marseille, France.

[**] We thank the French Ligue Nationale Contre le Cancer for awarding a research fellowship to O.R.

Supporting Information for this article is available on the WWW under http://www.angewandte.org or from the author.

  DOI: 10.1002/ange.200500700

of numerous physiologically active peptides.[5,6] NEP is expressed in a large variety of tissues including the brain, kidney, and lung,[7] but it is also overexpressed in various types of hematological tumors, particularly acute lymphoblastic leukemia[8] and some lymphomas, as well as in solid tumors such as melanoma,[9] colonic, pancreatic, and prostatic adenocarcinomas.[10] Presence, or absence, of NEP expression has been proposed as a prognostic indicator, depending on the tumor type.[11–17] In addition, lack of NEP expression in a prostatic carcinoma may predict decreased androgen sensitivity and a poorer response to hormonal deprivation therapy.[18,19] A noninvasive scintigraphic technique imaging tumor-cell accumulation of a labeled NEP inhibitor could be an interesting diagnosis and/or prognosis tool.

Structure–activity relationship studies of NEP inhibitors,[6] site-directed mutagenesis experiments,[6,20,21] and crystallographic studies of enzyme–inhibitor complexes further elucidated the interactions that stabilize substrates or inhibitors in the NEP active site. Potent inhibition of NEP is obtained with compounds containing a strong zinc ligand as a phosphinic group, a hydrophobic moiety interacting with the S'_1 subsite of the enzyme,[22] hydrogen-bonding donor and acceptor groups for binding with Asn542 and Arg717, and a carboxylate function for Arg102 recognition (Scheme 1).

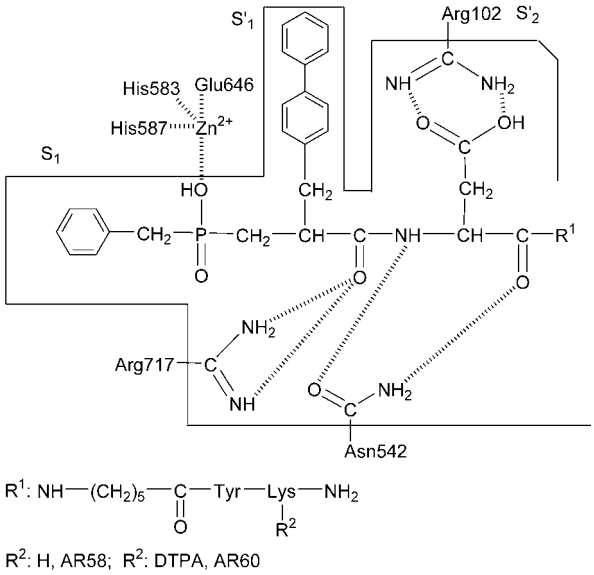

Scheme 1. Model of NEP active-site recognition by the phosphinic inhibitors AR58 and AR60 proposed from the crystallographic data reported by Oefner et al.[24]

Based on these findings, we designed novel compounds with a biphenylmethyl group and an aspartic acid unit to interact with the S'_1 and S'_2 subsites, respectively, and a benzyl moiety bearing a phosphinyl group as zinc ligand (Scheme 1). A 6-aminohexanoic acid was introduced as a spacer and its carboxylate moiety was coupled to a dipeptide amide Tyr-Lys-NH_2, with the tyrosine residue allowing labeling with iodine isotopes. The chelating agent diethylenetriaminepentaacetic acid (DTPA) was introduced on the ε NH_2 group of the lysine to allow labeling with metal radioisotopes. The peptide part of the molecule was synthesized by solid-phase methods and the phosphinic moiety, prepared independently by liquid-phase synthesis, was incorporated onto the peptidyl resin by a classical coupling step (Scheme 2, see the Supporting Information).

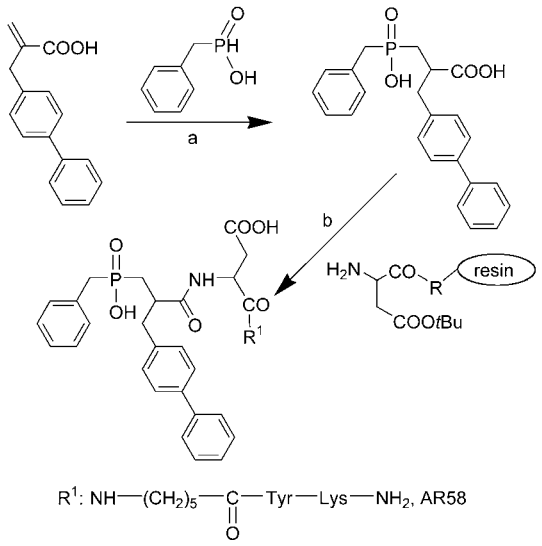

Scheme 2. Synthesis of the NEP inhibitor AR58. a) Bis(trimethylsilyl)-acetamide, 70°C; b) BOP, DIEA, NMP, solid-phase peptide synthesis then cleavage from the MBHA resin and final deprotection of the side chains of the amino acid residues (*tert*-butyl ether: Tyr, *tert*-butyl ester: Asp, *N-tert*-butoxycarbonyl: Lys) by trifluoroacetic acid to form R^1 and the desired product. BOP = 1-benzotriazolyloxytris(dimethylamino)-phosphonium hexafluorophosphate, DIEA = diisopropylethylamine, NMP = *N*-methyl-pyrrolidone, MBHA = 4-methyl-benzhydrylamine.

As the phosphinic moiety was synthesized as a mixture of enantiomers, the inhibitor was obtained as a mixture of two stereoisomers, which were separated by C18 reversed-phase HPLC. The first eluted isomer exhibited the best inhibitory potency: AR58-1 had an inhibition constant of $K_i = (3.6 \pm 0.1) \times 10^{-8}$ M, versus $K_i = (6.7 \pm 0.4) \times 10^{-7}$ M for the second eluted isomer (AR58-2).

High specific activities were obtained by labeling the DTPA-substituted derivative of AR58-1, referred to as AR60, with ^{111}In ((191 ± 20) MBq nmol^{-1}). The AR60 equilibrium binding-affinity constant ($(1.1 \pm 0.1) \times 10^8$ M^{-1}) was determined by competition binding experiments (Figure 1) on a human Burkitt lymphoma cell line (Ramos cells), in which NEP expression was confirmed by fluorescence-activated cell sorter (FACS) analysis (see the Supporting Information). This result suggests that coupling to DTPA does not significantly lower affinity. The number of NEP binding sites per Ramos cell (2.6×10^4–5.7×10^4) was in the same range as that already determined from equilibrium binding experiments of ^{125}I-labeled anti-CD10 antibody (2.1×10^4–7.5×10^4).[23]

A significant specific binding of ^{111}In-labeled AR60 to tissues of the kidneys (mainly the cortical zone), lungs, liver, and small intestine, but not of muscle, heart, stomach (not shown), and colon, was demonstrated by in vitro autoradiography studies (Figure 2), in agreement with NEP expression already described in these organs.[7] This labeled inhibitor

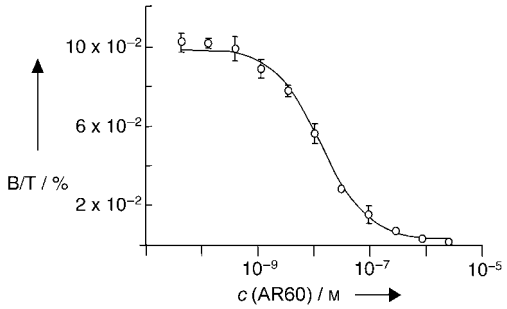

Figure 1. Typical competition binding curve between ^{111}In-labeled and unlabeled AR60. Trace amounts of ^{111}In-labeled AR60 were incubated with Ramos cells in the presence of increasing concentrations of AR60 saturated with nonradioactive indium. (The curve was generated by computer simulation with the Equilibrium Expert software.[25]) The fraction of radioactivity associated to the cells (bound/total (B/T) in %) was counted. The mean values from triplicate determinations are plotted. Bars give standard deviation values except those that were smaller than the points as plotted.

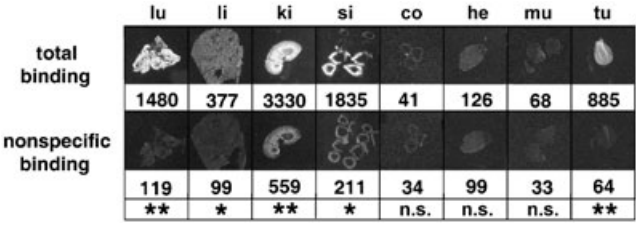

Figure 2. Autoradiogram of ^{111}In-AR60 binding to tissue sections (lu = lungs, li = liver, sp = spleen, ki = kidneys, si = small intestine, co = colon, he = heart, mu = muscle) from healthy BALB/c mice and intravenous grafts of Ramos cells to SCID mice (tu = tumor). Top: total binding. Bottom: nonspecific binding evaluated on adjacent sections in the presence of an excess (10^{-6} M) of AR58-1. Binding quantification, expressed in arbitrary activity units per surface unit, is indicated on each image. The Student t test was used to evaluate the significance of the results (*: statistical probability value $p < 0.05$; **: $p < 0.01$; n.s.: not significant).

bound specifically to sections of Ramos cell grafts to SCID mice.

We then investigated the in vivo biodistribution of ^{111}In-AR60 three and six hours after intravenous injection to healthy BALB/c mice (Figure 3). A fast blood clearance of ^{111}In-AR60 was observed, as assessed by the low residual blood radioactivity six hours after injection. Activity uptake was observed primarily in the kidneys and to a lesser extent in the lungs, liver, and colon. Since about 92% of the colon activity was associated with the stools, activity uptake in this organ was related to biliary excretion of ^{111}In-AR60. A low activity accumulation of < 1% of the injected dose per gram was observed in other organs six hours after injection. ^{111}In-AR60 stability in vivo was high since more than 70% was recovered intact in the serum 1 h after injection.

Coinjection of ^{111}In-AR60 (10 pmol) and a large excess of unlabeled Thiorphan (790 nmol), a specific NEP inhibitor, considerably reduced organ activity in the lungs, adrenal tissues, and kidneys, a result indicating uptake specificity in these organs (mean D values ± (standard error of the mean; s.e.m.) in the absence versus in the presence of thiorphan as

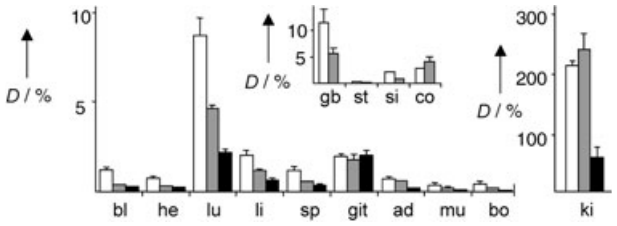

Figure 3. Biodistribution studies of ^{111}In-AR60 in healthy BALB/c mice. Mice were sacrificed, after an intravenous injection of only ^{111}In-AR60 (10 pmol in 150 μL of phosphate-buffered saline (PBS)) at 3 h (white bars) or 6 h (gray bars) or at 6 h in the presence of excess thiorphan (790 nmol, black bars). Tissue radioactivity is expressed as the percentage of injected dose per g of tissue (D, mean value ± standard error of the mean (s.e.m.), number of animals: 5 at 3 h, 4 at 6 h). Injected doses were corrected by subtraction of noninjected and subcutaneously injected material. Additional abbreviations to Figure 2: bl = blood, sp = spleen, git = gastrointestinal tract, ad = adrenal tissues, bo = bone, gb = gall bladder, st = stomach.

well as the p values: lungs: 4.60 ± 0.93 versus 2.17 ± 0.31, $p < 0.05$; adrenal tissues: 0.60 ± 0.08 versus 0.21 ± 0.03, $p < 0.01$; kidneys: 234 ± 56 versus 56 ± 33, $p < 0.01$;). Liver labeling was low and no significant difference was observed in the presence of thiorphan. These results are consistent with the rapid decrease of liver activity and the absence of gut activity through uptake of a tritiated NEP inhibitor, facts which suggest that several tissues are inaccessible to intravenously injected inhibitors thanks to the presence of functional barriers.[7]

^{111}In-AR60 uptake in tumors evaluated in SCID mice intravenously grafted with Ramos human Burkitt lymphoma cells was high ((10.3 ± 2.4) D, with a range of 21.8–3.5 D, 4.5 h after injection). Since in this model disseminated tumor-cell grafts occur in different organs, normal tissue uptakes were evaluated in healthy SCID mice. Tumor to normal tissue uptake ratios were high for the brain (144 ± 30, not shown), heart, stomach, blood, adrenal tissues, liver, spleen, and small intestine. Lower targeting contrasts were obtained for other organs, with values of around 3 for the colon, muscle, and bone, 1.4 ± 0.3 for the lungs, and 0.06 ± 0.01 for the kidneys (Figure 4).

Since the tumor to normal tissue uptake ratio is the key for isotopic tumor imaging, ^{111}In-AR60 should provide good contrast images except for tumors located on or near organs with high NEP expression, such as the kidneys and lungs. In

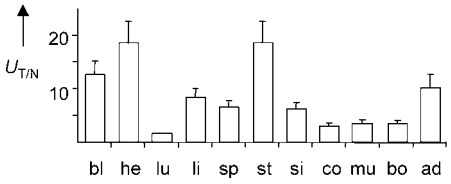

Figure 4. Tumor to normal tissue uptake ratios $U_{T/N}$ of ^{111}In-AR60 in SCID mice intravenously grafted with Ramos cells. Four animals were given ^{111}In-AR60 (10 pmol in 150 μL of PBS) by intravenous injection. Blood, organs, and tumor masses were collected and counted for radioactivity 4.5 h later. Tumor involvement of macroscopically suspect specimens was confirmed by histological analysis. Injected doses were corrected for losses as described in the legend to Figure 3. Since the graft is disseminated, results are expressed as the ratio between tumor uptake (10 samples) and mean organ uptake in nongrafted mice (mean value of $U_{T/N}$ ± (s.e.m.)).

some organs of tumor-bearing mice, with no macroscopic tumor involvement, activity uptake was greater than the mean uptake of corresponding organs of nongrafted mice. Histological analysis revealed tumor involvement in four of these samples, two brain samples with values of 0.78 and 0.57 *D* versus (0.07 ± 0.03) *D* in ungrafted mice and two adrenal tissue samples with values of 1.91 and 9.33 *D* versus (1.07 ± 0.39) *D* in ungrafted mice. These results further demonstrated the specificity of tumor uptake of ^{111}In-AR60.

In conclusion, the fast plasma clearance, the elevated tumor labeling, and the low nonspecific uptake of ^{111}In-labeled NEP ligand AR60 in normal organs provide high uptake ratios between tumor and normal organs except for the kidneys and lungs, which express high NEP levels. Noninvasive scintigraphic imaging of NEP expression with this compound may be a potential tool for the diagnosis and/or prognosis of different tumor types.

Received: February 24, 2005
Published online: May 31, 2005

Keywords: imaging agents · metalloenzymes · peptidomimetics · radiopharmaceuticals · tumor targeting

[1] D. Kwekkeboom, E. P. Krenning, M. de Jong, *J. Nucl. Med.* **2000**, *41*, 1704.
[2] M. De Jong, D. Kwekkeboom, R. Valkema, E. P. Krenning, *Eur. J. Nucl. Med. Mol. Imaging* **2003**, *30*, 463.
[3] S. Furumoto, K. Takashima, K. Kubota, T. Ido, R. Iwata, H. Fukuda, *Nucl. Med. Biol.* **2003**, *30*, 119.
[4] Q. H. Zheng, X. Fei, T. R. DeGrado, J. Q. Wang, K. L. Stone, T. D. Martinez, D. J. Gay, W. L. Baity, B. H. Mock, B. E. Glick-Wilson, M. L. Sullivan, K. D. Miller, G. W. Sledge, G. D. Hutchins, *Nucl. Med. Biol.* **2003**, *30*, 753.
[5] B. Malfroy, J. P. Swerts, A. Guyon, B. P. Roques, J. C. Schwartz, *Nature* **1978**, *276*, 523.
[6] B. P. Roques, F. Noble, V. Dauge, M. C. Fournie-Zaluski, A. Beaumont, *Pharmacol. Rev.* **1993**, *45*, 87.
[7] N. Sales, I. Dutriez, B. Maziere, M. Ottaviani, B. P. Roques, *Regul. Pept.* **1991**, *33*, 209.
[8] M. A. Shipp, J. Vijayaraghavan, E. V. Schmidt, E. L. Masteller, L. D'Adamio, L. B. Hersh, E. L. Reinherz, *Proc. Natl. Acad. Sci. USA* **1989**, *86*, 297.
[9] S. Carrel, L. Zografos, M. Schreyer, D. Rimoldi, *Melanoma Res.* **1993**, *3*, 319.
[10] P. Chu, D. A. Arber, *Am. J. Clin. Pathol.* **2000**, *113*, 374.
[11] M. Ponzoni, A. J. Ferreri, G. Pruneri, B. Pozzi, S. Dell'Oro, A. Pigni, G. Pinotti, E. Villa, M. Freschi, G. Viale, C. Capella, *Int. J. Cancer* **2003**, *106*, 288.
[12] T. Tokuhara, M. Adachi, H. Hashida, H. Ishida, T. Taki, M. Higashiyama, K. Kodama, S. Tachibana, S. Sasaki, M. Miyake, *Jpn. J. Thorac. Cardiovasc. Surg.* **2001**, *49*, 489.
[13] K. Iwaya, H. Ogawa, M. Izumi, M. Kuroda, K. Mukai, *Virchows Arch.* **2002**, *440*, 589.
[14] S. N. Gaidukova, L. A. Sivak, *Lik. Sprava* **2002**, 47.
[15] J. H. Go, W. I. Yang, H. J. Ree, *Arch. Pathol. Lab. Med.* **2002**, *126*, 956.
[16] P. Uherova, C. W. Ross, B. Schnitzer, T. P. Singleton, W. G. Finn, *Am. J. Clin. Pathol.* **2001**, *115*, 582.
[17] J. P. Vannier, M. C. Bene, G. C. Faure, C. Bastard, R. Garand, A. Bernard, *Br. J. Haematol.* **1989**, *72*, 156.
[18] S. J. Freedland, D. B. Seligson, A. Y. Liu, A. J. Pantuck, S. H. Paik, S. Horvath, J. A. Wieder, A. Zisman, D. Nguyen, C. L. Tso, A. V. Palotie, A. S. Belldegrun, *Prostate* **2003**, *55*, 71.
[19] C. N. Papandreou, B. Usmani, Y. Geng, T. Bogenrieder, R. Freeman, S. Wilk, C. L. Finstad, V. E. Reuter, C. T. Powell, D. Scheinberg, C. Magill, H. I. Scher, A. P. Albino, D. M. Nanus, *Nat. Med.* **1998**, *4*, 50.
[20] N. Dion, P. Cohen, P. Crine, G. Boileau, *FEBS Lett.* **1997**, *411*, 140.
[21] A. Devault, V. Sales, C. Nault, A. Beaumont, B. Roques, P. Crine, G. Boileau, *FEBS Lett.* **1988**, *231*, 54.
[22] I. Schechter, A. Berger, *Biochem. Biophys. Res. Commun.* **1967**, *27*, 157.
[23] M. Hillairet de Boisferon, O. Raguin, M. Dussaillant, W. Rostene, J. Barbet, A. Gruaz-Guyon, *Bioconjugate Chem.* **2000**, *11*, 452.
[24] C. Oefner, B. P. Roques, M. C. Fournie-Zaluski, G. E. Dale, *Acta Crystallogr. D Biol. Crystallogr.* **2004**, *60*, 392.
[25] O. Raguin, A. Gruaz-Guyon, J. Barbet, *Anal. Biochem.* **2002**, *310*, 1.

